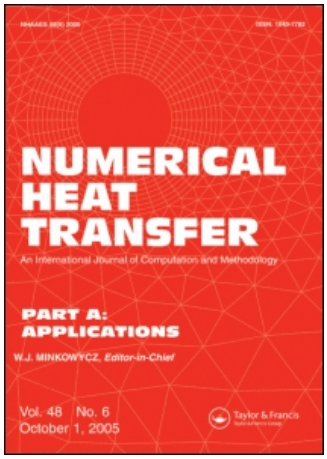
This article was downloaded by:[Dewan, Anupam]
On: 15 April 2008
Access Details: [subscription number 792147675]
Publisher: Taylor & Francis
Informa Ltd Registered in England and Wales Registered Number: 1072954
Registered office: Mortimer House, 37-41 Mortimer Street, London W1T 3JH, UK



Numerical Heat Transfer, Part A: Applications
An International Journal of Computation and Methodology
Publication details, including instructions for authors and subscription information:
http://www.informaworld.com/smpp/title~content=t713657973

Distribution of Temperature as a Passive Scalar in the Flow Field of a Heated Turbulent Jet in a Crossflow

Manabendra Pathak [a]; Anupam Dewan [a]; Anoop K. Dass [a]
[a] Department of Mechanical Engineering, Indian Institute of Technology Guwahati, Guwahati, India

Online Publication Date: 01 January 2008
To cite this Article: Pathak, Manabendra, Dewan, Anupam and Dass, Anoop K. (2008) 'Distribution of Temperature as a Passive Scalar in the Flow Field of a Heated Turbulent Jet in a Crossflow', Numerical Heat Transfer, Part A: Applications, 54:1, 67 - 92
To link to this article: DOI: 10.1080/10407780802025143
URL: http://dx.doi.org/10.1080/10407780802025143

PLEASE SCROLL DOWN FOR ARTICLE

Full terms and conditions of use: http://www.informaworld.com/terms-and-conditions-of-access.pdf

This article maybe used for research, teaching and private study purposes. Any substantial or systematic reproduction, re-distribution, re-selling, loan or sub-licensing, systematic supply or distribution in any form to anyone is expressly forbidden.

The publisher does not give any warranty express or implied or make any representation that the contents will be complete or accurate or up to date. The accuracy of any instructions, formulae and drug doses should be independently verified with primary sources. The publisher shall not be liable for any loss, actions, claims, proceedings, demand or costs or damages whatsoever or howsoever caused arising directly or indirectly in connection with or arising out of the use of this material.

Numerical Heat Transfer, Part A, 54: 67–92, 2008
Copyright © Taylor & Francis Group, LLC
ISSN: 1040-7782 print/1521-0634 online
DOI: 10.1080/10407780802025143

Downloaded By: [Dewan, Anupam] At: 05:36 15 April 2008

DISTRIBUTION OF TEMPERATURE AS A PASSIVE SCALAR IN THE FLOW FIELD OF A HEATED TURBULENT JET IN A CROSSFLOW

Manabendra Pathak, Anupam Dewan, and Anoop K. Dass
Department of Mechanical Engineering, Indian Institute of Technology Guwahati, Guwahati, India

This article presents a computational investigation of the mean flow field of heated turbulent rectangular jets in a crossflow. The jet is discharged with a slightly higher temperature (about 6°C) than the crossflow. The computations are carried out for two values of jet-to-crossflow velocity ratio, 6 and 9. The commercial code FLUENT 6.2.16, employing the Reynolds stress transport model, is used to predict the mean flow field. The influence of the velocity field on the temperature distributions is discussed. A comparison of the predicted results is made with the available experimental data, and reasonably good agreement is observed.

1. INTRODUCTION

The problem of jets in crossflow is important from both theoretical and practical application points of view. Theoretically, the flow field is very complex, as the interaction and mixing between the jet and the crossflow take place at different scales with intricate unsteadiness. The flow field is characterized by four different types of vortices: the jet shear layer vortex, horseshoe vortex, wake vortex, and counter-rotating vortex pair [1–3]. These vortices play a dominant role in the complex mechanisms of mixing and interaction between the jet and the crossflow. In applications, the problem of jets in crossflow is found either under isothermal conditions or for a heated/cold jet in crossflow. The flow field of a heated jet in cold crossflow is encountered in many engineering and environmental problems, such as exhaust gas issuing from the exhaust stacks of most industrial plants, exhaust gas from vehicles and effluent from plants discharged into rivers, etc. In all these applications, it is found that jets and plumes are either discharged vertically or at an angle to the crossflow. In investigations of such problems, the interactions between the jet and the crossflow, the resulting temperature downstream of the jet, the thermal spread or the trajectory, and the physical path of the jet are extremely important factors. In many situations the temperature field is strongly affected by the velocity field and can be regarded as a passive scalar. In such conditions it is necessary to understand the mean and fluctuating characteristics of the thermal spread and mixing

Received 23 July 2007; accepted 1 February 2008.
Address correspondence to Anupam Duwan, Department of Mechanical Engineering, Indian Institute of Technology Guwahati, Guwahati 781039. E-mail: adewan@iitg.ernet.in

Downloaded By: [Dewan, Anupam] At: 05:36 15 April 2008

NOMENCLATURE

D	width of the jet	w	mean velocity along the spanwise (z) direction
g	acceleration due to the gravity	x	coordinate along the crossflow direction
k	turbulent kinetic energy	y	coordinate along the direction of the jet discharge
n	coordinate perpendicular to the jet trajectory	z	coordinate along the spanwise direction
p	mean pressure	ε	rate of dissipation of turbulent kinetic energy k
R	jet-to-crossflow velocity ratio (v_j/u_a)	ν_t	eddy viscosity
R_{bj}	exit Richardson number	ρ	density
s	distance along the jet trajectory from the center of the jet slot	σ_ε	model constant
T	mean temperature	σ_k	model constant
T_i	mean temperature at the crossflow inlet	σ_t	turbulent Prandtl number
T_j	mean temperature of the jet	**Subscripts**	
u	mean velocity along the crossflow (x) direction	a	crossflow condition
u_a	crossflow velocity	i, j, k	tensor notation
v	mean velocity along the jet discharge (y) direction	j	condition at the jet discharge
v_j	jet velocity		

between the jet and the crossflow. Several researchers [4–13] have reported the flow behavior and heat transfer analysis of a heated jet in crossflow. In most of these studies the gross temperature field and the detailed correlations for predicting the temperature distributions and the relevant parametric variations at downstream of the jets are provided.

Sherif and Pletcher [8] investigated experimentally the flow field of a round heated jet in a crossflow for velocity ratios of 1, 2, 4, and 7. They mainly studied the jet wake thermal characteristics and observed the qualitative differences of the flow behavior for small velocity ratios ($R < 2$) and large velocity ratios ($R > 2$). Based on their observations, they suggested that the velocity ratio $R = 2$ should be a borderline between the high and low velocity ratios.

Much of the work reported in the literature concerns the flow field of round jets in crossflow. There is only few literature reporting the flow field of square or rectangular heated jets in crossflow. The flow field of a two-dimensional (2-D) heated plane jet in a crossflow, where the jet was confined in a channel, was investigated experimentally by Chen and Hwang [7]. In this flow configuration, the jet was injected from a narrow slot developed between the two side walls of the channel, without any clearance between the jet and walls. Chen and Hwang [7] reported the two-dimensionality of the flow field, especially at the center of the slot. Nishiyama et al. [9] investigated the characteristics of the temperature fluctuations in a slightly heated 2-D jet issuing through a slot normally into a crossflow for various velocity ratios. They studied the effects of the velocity ratio on the mean and fluctuating temperature fields. They observed that the low-velocity-ratio jets behave like a wall jet and the high-velocity-ratio jets are liftoff jets with a recirculation region. Ramaprian and Haniu [4] and Haniu and Ramaprian [5] investigated experimentally the flow

Downloaded By: [Dewan, Anupam] At: 05:36 15 April 2008

field of turbulent plane jets in a narrow channel crossflow. They performed the experiments for three values of jet-to-crossflow velocity ratio, $R = 6$, 9, and 10, for both isothermal and heated jets. They performed the measurements of mean and turbulent flow properties in the middle of the jet slot and did not report any observation in the other spanwise planes and near-bottom-wall regions. They reported about the two-dimensionality of the flow field near the jet central plane area.

In recent years, besides the investigations of velocity and vorticity fields, investigation of the scalar field of transverse jets has also received some attentions. Mean scalar fields in terms of concentration were measured experimentally by Niederhaus et al. [14], who applied planar laser-induced fluorescence (PLIF) to obtain the scalar concentration fields in the cross sections of crossflowing jets in water, with velocity ratio $R = 4.9$ to 11.1. Smith and Mungal [15] applied PLIF to investigate air-into-air crossflowing jets and mapped the concentration field in the cross-sectional planes, in the symmetry plane, and in planes parallel to the jet exit plane, for velocity ratios ranging from 5 to 20. They also measured the vortex interaction region, mean trajectories and concentration decay, and overall structural features of mixing of a round jet in a crossflow. Su and Mungal [16] performed a comprehensive investigation of the scalar and velocity fields in the developing region of a crossflowing turbulent jet in the gas phase, using the planar imaging technique for the velocity ratio $R = 5.7$. Their results showed that the intensity of the mixing, as quantified by the scalar variance and the magnitude of the turbulent scalar fluxes, is initially higher on the jet windward side, but eventually becomes higher on the wake side. Plesniak and Cusano [17] performed an experimental investigation of a confined rectangular jet in a crossflow to investigate the scalar mixing. They systematically varied three pertinent parameters, i.e., the momentum ratio, injection angle, and development length. They observed the three regimes (wall jet, fully lifted jet, and reattached jet) for the jet crossflow interaction and the resulting concentration fields. Their combined scalar concentration and velocity data provided an understanding of the large-scale mixing and the role of coherent structures and their evolution. Recently, Shan and Dimotakis [18] investigated the Reynolds number dependence of the scalar mixing by examining the probability distribution of the jet fluid in strong liquid-phase transverse jets at a fixed far-downstream location. In their study, the mixing at high Schmidt number was compared between the transverse and free jets to investigate the possible differences in mixing for fully developed (but finite Reynolds number) turbulent flows.

The literature review reveals that although much of the computational work on jets in crossflow have been made using relatively simple turbulence models such as the k–ε model, in most cases, the predictions by these simple models result in poor agreement with the experimental results [19–21]. The Reynolds stress transport (RST) model is known to work better than the standard k–ε model in investigating flow fields that are highly anisotropic and characterized by streamline curvature effects such as the flow field of jets in crossflow [22]. Demuren [22] has observed that a RST model reproduces peak vorticity and counter-rotating vortice pair (CRVP) strength very well and predicts Reynolds stresses better than those predicted by the standard k–ε model. Moreover, this model is computationally much less expensive than the use of either large-eddy simulation or direct numerical simulation. Said

Downloaded By: [Dewan, Anupam] At: 05:36 15 April 2008

et al. [13] performed a numerical investigation of a round heated jet in a crossflow using various turbulence models. They also observed better performance of the RST model compared to the two-equation models. Hale et al. [23] investigated the surface heat transfer associated with a row of multiple round short-hole jets in a crossflow using the commercial flow solver FLUENT. They employed a RST model with nonequilibrium wall functions and a two-layer zonal approach in their code, and they observed better performance with the two-layer zonal model than with the RST model. However, no work on the study of rectangular heated jets in crossflow using the RST model has been reported in the literature.

In the present work, the flow field and temperature distribution of a slightly heated jet in crossflow is investigated computationally for the two velocity ratios of jet and crossflow $R = 6$ and 9. The length of the jet discharge slot spans more than 55% of the crossflow channel width, rather than issuing into a semiconfined or unconfined crossflow. This flow configuration has so for not been studied in detail. The computations are carried out using the commercial code FLUENT 6.2.16, based on the finite-volume method and employing the RST model. The predicted results are compared with the experimental data of Ramaprian and Haniu [4] and Haniu and Ramaprian [5] reported at the central plane. The objective of the present investigation is to provide more detailed information about the flow and thermal characteristics than that given in [4, 5] experimentally. The present work also investigates the influence of the velocity field on the distribution of the temperature as a passive scalar. A description of the computational domain, governing equations, turbulence model, and computational methodology is presented in Section 2. The predictions of the mean and turbulent quantities and their comparisons with the measurements are described in Section 3, followed by conclusions in Section 4.

2. PROBLEM FORMULATION

A schematic diagram of the three-dimensional (3-D) computational domain and the coordinate system used in the present work is shown in Figure 1. The origin is located at the center of the jet slot. The x coordinate represents the distance in the cross-stream direction, y the vertical, and z the spanwise direction. The size of the computational domain depends on the value of the jet-to-crossflow velocity ratio R. The sizes of the computational domain (Figure 1) used for different values of R are shown in Table 1.

2.1. Governing Equations

The Reynolds-averaged continuity, three momentum equations, and energy equation are the governing equations. We assumed the flow to be steady in mean. The equations may be expressed using the Cartesian tensor notation as follows.
Continuity:

$$\frac{\partial}{\partial x_j} u_j = 0 \tag{1}$$

Downloaded By: [Dewan, Anupam] At: 05:36 15 April 2008

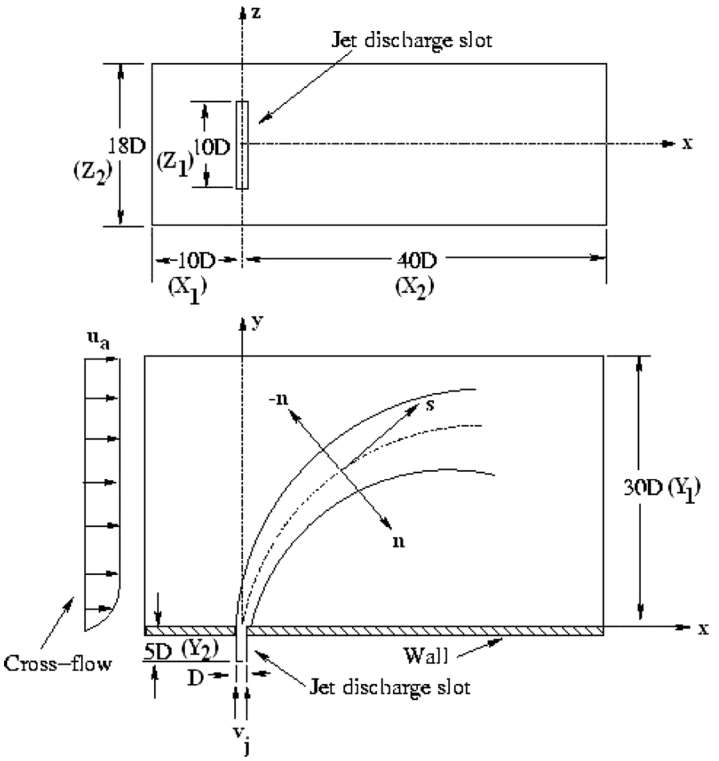


Figure 1. Schematic diagram of the computational domain for $R = 6$.

Momentum:

$$\frac{\partial}{\partial x_j}(u_i u_j) = -\frac{\partial p}{\rho \partial x_i} + \frac{\partial}{\partial x_j}\left(-\overline{u_i' u_j'}\right) \tag{2}$$

Energy:

$$\frac{\partial (u_j T)}{\partial x_j} = \frac{\partial}{\partial x_j}\left(\frac{\nu_t}{\sigma_t}\frac{\partial T}{\partial x_j}\right) \tag{3}$$

Here u_i denote the mean velocities, p the mean pressure, and T the mean temperature. σ_t denotes turbulent Prandtl number and is defined as the ratio of the thermal diffusivity and eddy diffusivity. In many applications one can get results of modest

Table 1. Domain size for different values of R

R	X_1 (x/D)	X_2 (x/D)	Y_1 (y/D)	Y_2 (y/D)	Z_1 (z/D)	Z_2 (z/D)
6	10	40	30	5	10	18
9	10	50	40	5	10	18

Downloaded By: [Dewan, Anupam] At: 05:36 15 April 2008

accuracy by using a constant value of σ_t [24]. The value of the turbulent Prandtl number used in the present work is 0.85.

It is to be noted that the jet discharge and the flow in the entire computational domain are assumed to be fully turbulent and thus independent of the value of the Reynolds number. The discharged jet is at a slightly higher temperature than that of the crossflow, with a temperature difference of 5.7°C for the velocity ratio $R = 6$ and 6.1°C for $R = 9$ according to the experimental conditions [4, 5]. The value of the exit buoyancy Richardson number ($R_{bj} = \Delta\rho_j g D/\rho_a v_j$) due to the heating is quite low, thus ensuring a negligible buoyancy effect with temperature playing the role of a passive scalar only. A physical quantity that is transported by the flow but in turn does not alter the flow field is called a passive scalar. In such a condition, a passive scalar such as the temperature is transported only by the forced-convective flow. It is logical to use the momentum ratio ($= \rho_j v_j^2/\rho_a u_a^2$) in the formulation of investigation of a heated jet in crossflow, but since both the jets and crossflow are of the same fluid (water), the change of density for a small temperature difference was assumed to be negligible. Thus the momentum ratio is equivalent to the square of the velocity ratio.

2.2. Turbulence Model: Reynolds-Stress Transport Model

Transport equations for six individual components of Reynolds stresses ($\overline{u_i' u_j'}$) are solved numerically. The exact equations for the stresses used in the present investigation can be written in tensor notation as

$$\underbrace{\frac{\partial}{\partial x_k}(u_k \overline{u_i' u_j'})}_{C_{ij}=\text{convection}} = \underbrace{-\frac{\partial}{\partial x_k}\left[\overline{u_i' u_j' u_k'} + \overline{p'(\delta_{kj} u_i' + \delta_{ik} u_j')}\right]}_{D_{ij}^T=\text{turbulent diffusion}} \underbrace{- \left(\overline{u_i' u_k'}\frac{\partial u_j}{\partial x_k} + \overline{u_j' u_k'}\frac{\partial u_i}{\partial x_k}\right)}_{P_{ij}=\text{stress production}} + \underbrace{\frac{p'}{\rho}\overline{\left(\frac{\partial u_i'}{\partial x_j} + \frac{\partial u_j'}{\partial x_i}\right)}}_{\phi_{ij}=\text{pressure strain}} \underbrace{- 2\nu_t \overline{\frac{\partial u_i'}{\partial x_k}\frac{\partial u_i'}{\partial x_k}}}_{\varepsilon_{ij}=\text{dissipation}} \tag{4}$$

Since the jet discharge and the flow in the entire computational domain are assumed to be fully turbulent, the effect of the molecular viscosity is assumed to be negligible, and therefore the molecular diffusion term is neglected.

To obtain the boundary conditions for the Reynolds stresses at the different boundary zones, the equation for the turbulent kinetic energy (k) is solved. Moreover, the equation for the dissipation rate is solved to obtain the dissipation rate ε_{ij} of the Reynolds stress tensor. In both equations, a few minor modifications are made to the original form of the equations. The equations used are

$$\frac{\partial}{\partial x_i}(k u_i) = \frac{\partial}{\partial x_j}\left(\frac{\nu_t}{\sigma_k}\frac{\partial k}{\partial x_j}\right) + \frac{1}{2}P_{ii} - \varepsilon \tag{5}$$

Downloaded By: [Dewan, Anupam] At: 05:36 15 April 2008

$$\frac{\partial}{\partial x_i}(\varepsilon u_i) = \frac{\partial}{\partial x_j}\left(\frac{\nu_t}{\sigma_\varepsilon}\frac{\partial \varepsilon}{\partial x_j}\right) + \frac{1}{2}C_{\varepsilon 1}P_{ii}\frac{\varepsilon}{k} - C_{\varepsilon 2}\frac{\varepsilon^2}{k} \tag{6}$$

where P_{ii} is the production of k and $\sigma_k = 0.82$, $\sigma_\varepsilon = 1.0$, $C_{\varepsilon 1} = 1.44$, $C_{\varepsilon 2} = 1.92$ are the model constants. Although Eq. (5) is solved globally throughout the computational domain, the values of k obtained are used only for the boundary conditions. In other part of the flow domain, k is obtained by taking the trace of the Reynolds stress tensor: $k = 1/2\overline{u_i' u_i'}$.

2.2.1. Modeling different terms of Reynolds stress equation. Among the various terms of the Reynolds stress transport equation (4), the convection term (C_{ij}) and the production term (P_{ij}) do not require any modeling. However, the turbulent diffusion term (D_{ij}^T), the pressure strain term (ϕ_{ij}), and the dissipation term (ε_{ij}) need to be modeled to close the set of governing equations.

The turbulent diffusion term (D_{ij}^T) is modeled as suggested by Lien and Leschziner [25]. The pressure strain term (ϕ_{ij}) is generally modeled in FLUENT with a linear pressure strain model. However, the highly anisotropic nature of the flow due to the streamline curvature near the jet discharge, resulting from a strong interaction between the jet discharge and the crossflow, suggests that the production term and the pressure strain correlation play a dominant role in the prediction of the turbulent stresses. The pressure strain is especially important in producing the anisotropy of normal stress components. The quadratic pressure strain model proposed by Speziale et al. [26], which is known to improve the accuracy of a flow field with streamline curvature, is used to model the pressure strain term of the Reynolds stress transport equation (4). The dissipation term ε_{ij} is modeled in terms of the dissipation rate ε of turbulent kinetic energy as proposed by Sarkar and Balakrishnan [27].

2.3. Boundary Conditions

The boundary conditions used in the present computations are the inlet, outlet, and wall. The boundary condition at the inlet corresponds to the crossflow condition, i.e., the only component of the flow is along the crossflow direction ($u = u_a$), with zero components along both the vertical ($v = 0$) and spanwise directions ($w = 0$). The crossflow inlet boundary-layer thickness is set to $1.5D$ by adapting the boundary at the velocity inlet zone to match with the experimental conditions. Inside the boundary layer, the 1/7th power-law profile is used for the u-velocity component. A user-defined function (UDF) is used to introduce this profile at the inlet. The values of turbulent quantities at the crossflow inlet are based on the turbulent specification method, where the turbulent intensity and a length scale are prescribed. The value of the turbulent kinetic energy is taken from the 5% turbulent intensity based on the experimental data. The domain length in the vertical direction is used as the length scale to represent the turbulent dissipation rate. The values of Reynolds stresses at the flow inlet are taken from the prescription of the turbulent kinetic energy by assuming the isotropy of the turbulence as $\overline{u_i'^2} = 2/3k$, $\overline{u_i' u_j'} = 0$. The nondimensionalized temperature of 0.9813 for $R = 6$ or 0.9800 for $R = 9$ is specified at the crossflow inlet, which is maintained at a temperature of 300 K.

Downloaded By: [Dewan, Anupam] At: 05:36 15 April 2008

At the top surface, excluding the side-wall top, the free-stream condition is imposed and the values of u, v, w, k, and ε specified are the same as those at the inlet boundary. The tops of the side walls are treated as the wall. At the outlet plane, the normal gradients of all variables are assumed to be zero $[\partial f/\partial x = 0; f = (u, v, w, k, \varepsilon)]$. The whole bottom surface, excluding the jet discharge slot, is considered as a solid wall. The no-slip condition is applied there, and the standard wall functions are used to resolve the near-wall turbulence. The value of ${y_p}^+$ is taken as 11.3, above which the log-law is assumed to be valid. For the turbulent kinetic energy, a zero value is specified at the wall, while the value of dissipation at the near-wall point is set using a local equilibrium assumption as $\varepsilon = c_\mu^{3/4} k^{3/2}/(\delta y)$, where δy is the wall-normal grid spacing for the first grid point. To define the thermal boundary conditions at the wall, FLUENT has different types of thermal conditions such as fixed heat flux, fixed temperature, convective heat transfer, etc. In the present work a fixed temperature is applied at the wall. The nondimensionalized temperature of the wall is set in the same way as described in the crossflow inlet boundary condition ($= 300$ K).

The boundary conditions at the entry to the jet channel or jet plenum are $u = 0$, $w = 0$, and $v = v_j$. The value of turbulent kinetic energy is based on 6.5% turbulent intensity ($k = 0.00625 v_j^2$), and the value of the dissipation rate is taken using the expression proposed by Versteeg and Malaleskara [28], as $\varepsilon = c_\mu^{3/4}(k^{3/2}/0.5D)$. The nondimensionalized temperature corresponding to the value of temperature 305.7 K for $R = 6$ or 306.1 K for $R = 9$ was set as the jet-stream temperature at the inlet. Both side walls are treated with the no-slip condition, and the standard wall functions are used to resolve the near-wall turbulence.

2.4. Computational Methodology

In the present computation, a nonuniform staggered grid is used. The grid is clustered near the bottom wall in the y direction as well as near both side walls in the z direction. Moreover, grids are clustered at the jet exit region in the x direction. A staggered grid arrangement is employed in which the scalar variables (p, k, and ε) are positioned at the center of the control volume and the velocity components are positioned at the cell face. The momentum equations are discretized using the second-order upwind scheme, and all transport equations are discretized using the power-law scheme. The SIMPLE algorithm is used for coupling the pressure–velocity fields. The segregated solution method of FLUENT is employed, where each discrete governing equation is linearized implicitly with respect to the equation's dependent variable and which results in a linear system of equations. All the variables (u, v, w, k, and ε) are underrelaxed in each iteration. The solution is assumed to be converged when the normalized residual of the energy equation is less than 10^{-6} and the normalized residuals of continuity and other variables are less than 10^{-3}. The computations are performed on a Pentium 4 machine with 512 MB RAM, 1.6-GHz processor speed, and it takes approximately 34 days of CPU time to obtain the converged solution.

The present FLUENT code is validated by testing the present computations with the result reported by Hoda et al. [29], who performed numerical investigations

Downloaded By: [Dewan, Anupam] At: 05:36 15 April 2008

for a square jet in a crossflow for the velocity ratio of 0.5 using two versions of the RST model and large-eddy simulation (LES). For the validation, the present FLUENT code employed the Daly and Harlow [30] model for modeling the turbulent diffusion term of the RST equation, and the pressure strain term is modeled using the quadratic pressure strain model. Moreover, the wall reflection correction term is also included in the code, to meet the conditions of Hoda et al. [29]. A comparison of the predicted results of the cross-stream component of the mean velocity at a location $x/D = 3$, $z/D = 0$, for the velocity ratio $R = 0.5$ by the present code with the results of Hoda et al. [29] is shown in Figure 2. The agreement between the two predictions is fairly good, and the maximum difference between the two is 11.5%.

The grid sensitivity test of the present computation is conducted by using four different sets of grids, viz., $100 \times 75 \times 45$ (100 along x, 75 along y, and 45 along z directions), $130 \times 85 \times 55$, $140 \times 90 \times 60$, and $150 \times 95 \times 65$ by comparing the cross-stream component of the mean velocity (u/v_j) profile for $R = 6$. The velocity profiles for $R = 6$ at the plane $z/D = 0$ and at the location $x/D = 2$ is shown in Figure 3. It is observed that the grid refinement in general improves the prediction by reducing the higher prediction in the near-wall region and increasing the peak value of the jet velocity. The deviation among the predictions using the four different grids decreases as the mesh is refined, and the difference between the computations using the grid sizes of $150 \times 95 \times 65$ and $140 \times 90 \times 60$ is 3.4%. The results that are presented in the subsequent sections for the velocity ratio $R = 6$ are obtained using the grid size of $150 \times 95 \times 65$.

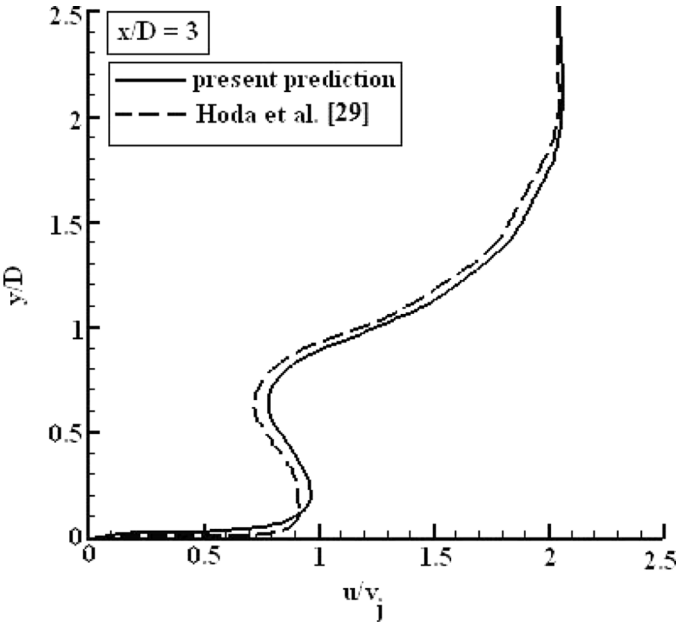


Figure 2. Comparison of the present prediction with the results of Hoda et al. [29] for the velocity ratio $R = 0.5$, $z/D = 0$.

Downloaded By: [Dewan, Anupam] At: 05:36 15 April 2008

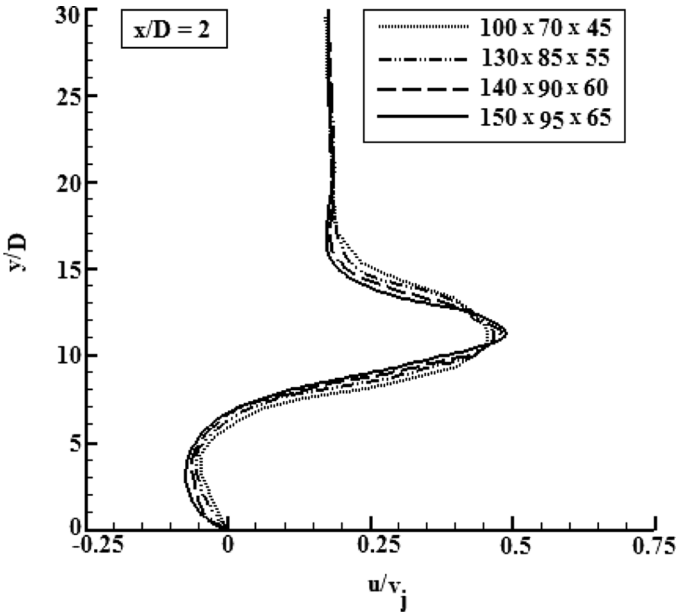


Figure 3. Grid sensitivity test: predicted cross-stream component of the mean velocity (u/v_j) profile for $R = 6$, $z/D = 0$.

3. RESULTS AND DISCUSSION

In the present work, computations are performed in Cartesian coordinates and the computed data are subsequently transformed to s–n coordinates for the purpose of comparison with the experimental data [4, 5]. To gain an understanding of the flow physics in a clear way and to provide the flow properties near the bottom wall, first we present the predictions of the mean flow properties in Cartesian coordinates.

3.1. Components of Mean Velocity

The mean velocity of the deflected jet can be considered as having three components, one along the x axis (in the direction of the crossflow), one along the y axis (in the direction of the jet discharge), and the third along the z axis (in the transverse direction). These three components are termed the cross-stream, vertical, and spanwise, respectively. All three components have significant contribution to the resultant mean flow field in the flow configuration considered in the present work.

Figure 4 shows the variation of the cross-stream component of the mean velocity (u/v_j) with distance from the wall (y/D) at various downstream positions (x/D) for the velocity ratio $R = 6$ at two spanwise planes at $z/D = 0$ and 6. The velocity profile at the jet central plane $(z/D = 0)$ is shown at five different downstream (x/D) positions in Figure 4*a*. A reverse flow region is formed near the wall, just at the downstream of the jet $(x/D = 2)$ by showing negative velocity. A weak wall-jet-like structure is observed near the bottom wall in the downstream positions $(x/D = 5$ and 10). Since the crossflow is weak in this case, the wall-jet-like structure

Downloaded By: [Dewan, Anupam] At: 05:36 15 April 2008

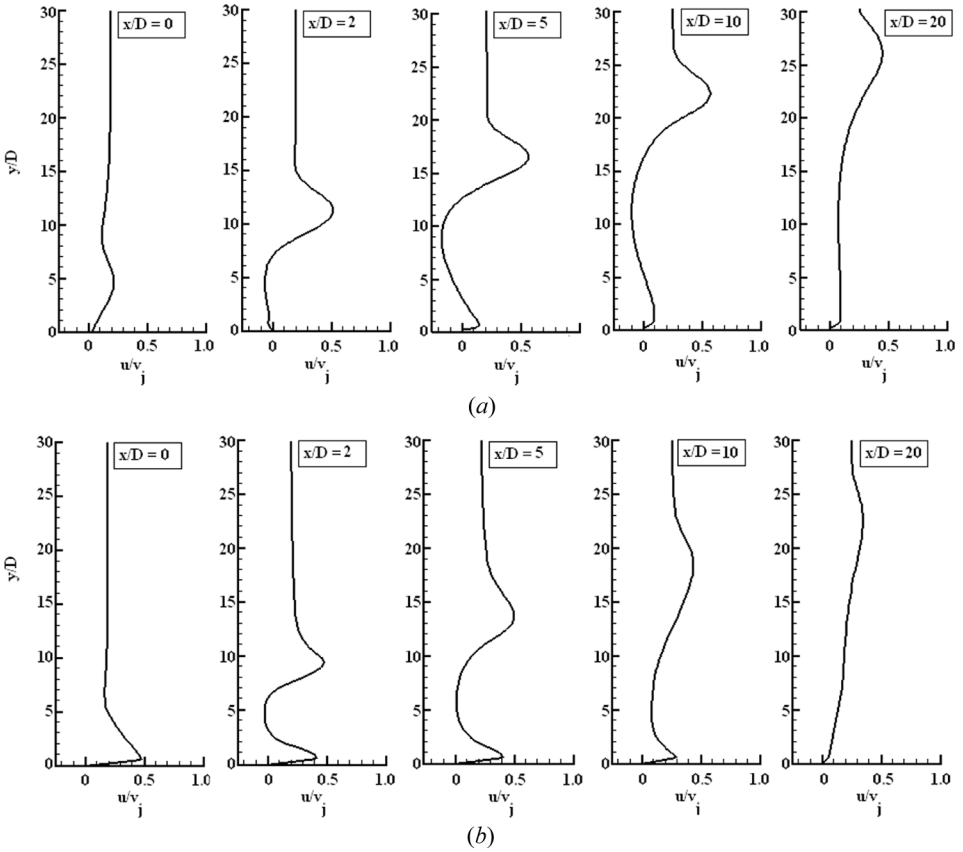


Figure 4. Prediction of the cross-stream component of the mean velocity at different downstream locations for $R = 6$: (*a*) $z/D = 0$; (*b*) $z/D = 6$.

is weak compared to the case of a strong crossflow, i.e., low values of the velocity ratio R [31, 32]. A wake region with a low velocity is observed above the wall jet shear layer. Also, a shear layer with strong velocity gradient above the wake region is observed at the locations of $x/D = 2$, 5, and 10. The size of the wake region is comparatively larger than that reported in [31, 32] for low values of R. The velocity gradient in the wake region and jet shear layer is diminished at the far downstream location ($x/D = 20$), and the flow recovers toward a boundary-layer profile.

To show the change of the velocity profile as one moves from the jet central plane ($z/D = 0$) toward the side wall, the velocity profile (u/v_j) is presented at $z/D = 6$ in Figure 4*b*. A qualitative difference in the trends of profiles is observed in this plane. The velocity profiles at all downstream locations are observed, as expected, to be different from those at the central plane ($z/D = 0$). The vertical height where the jet peak value occurs is less in this plane ($z/D = 6$) compared to that at the central plane. The size of the wakelike region is slightly smaller than that in the earlier case. Near the bottom wall, the wall-jet-like layer is prominent at all downstream locations, and it is even formed at $x/D = 0$ with steep velocity gradients.

Downloaded By: [Dewan, Anupam] At: 05:36 15 April 2008

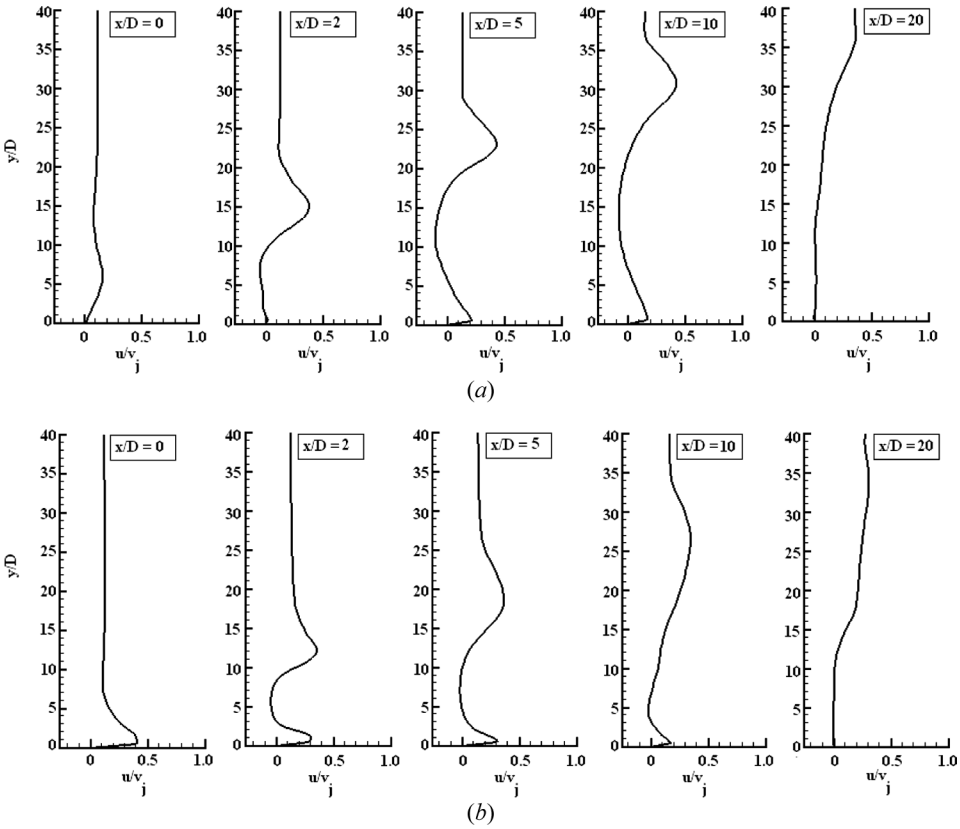


Figure 5. Prediction of the cross-stream component of the mean velocity at different downstream locations for $R = 9$: (*a*) $z/D = 0$; (*b*) $z/D = 6$.

The cross-stream component of the mean velocity profile (u/v_j) at two transverse planes (z/$D = 0$ and 6) and at different downstream locations ($x/D = 0$, 0, 2, 5, 10, and 20) for the velocity ratio $R = 9$ is shown in Figure 5. The peak values of the cross-stream components are seen at higher values of y/D in Figures 5*a* and 5*b* compared to the case of jet with $R = 6$ (Figures 4*a* and 4*b*). Thus the penetration height of the jet into the crossflow is observed more in this case compared to the case with $R = 6$. In this case also, qualitative differences in the velocity profiles are observed at the spanwise plane $z/D = 6$ than that at the plane $z/D = 0$.

Figure 6 shows the predictions of the vertical component of the mean velocity at different transverse planes and at different downstream positions for the velocity ratio $R = 6$. The downstream development of the vertical component of the mean velocity in the jet central plane ($z/D = 0$) is shown in Figure 6*a*. It is observed that at the jet discharge point ($x/D = 0$), the vertical component of the velocity is largely unaffected by the crossflow up to a height of about $y/D = 3$, showing a high value of the vertical component. Thus, until that point the jet is almost vertical. After a certain height, the jet is deflected and therefore the value of the vertical velocity component is reduced. Downstream of the jet slot (at $x/D = 2$), a weak wall jet flow

Downloaded By: [Dewan, Anupam] At: 05:36 15 April 2008

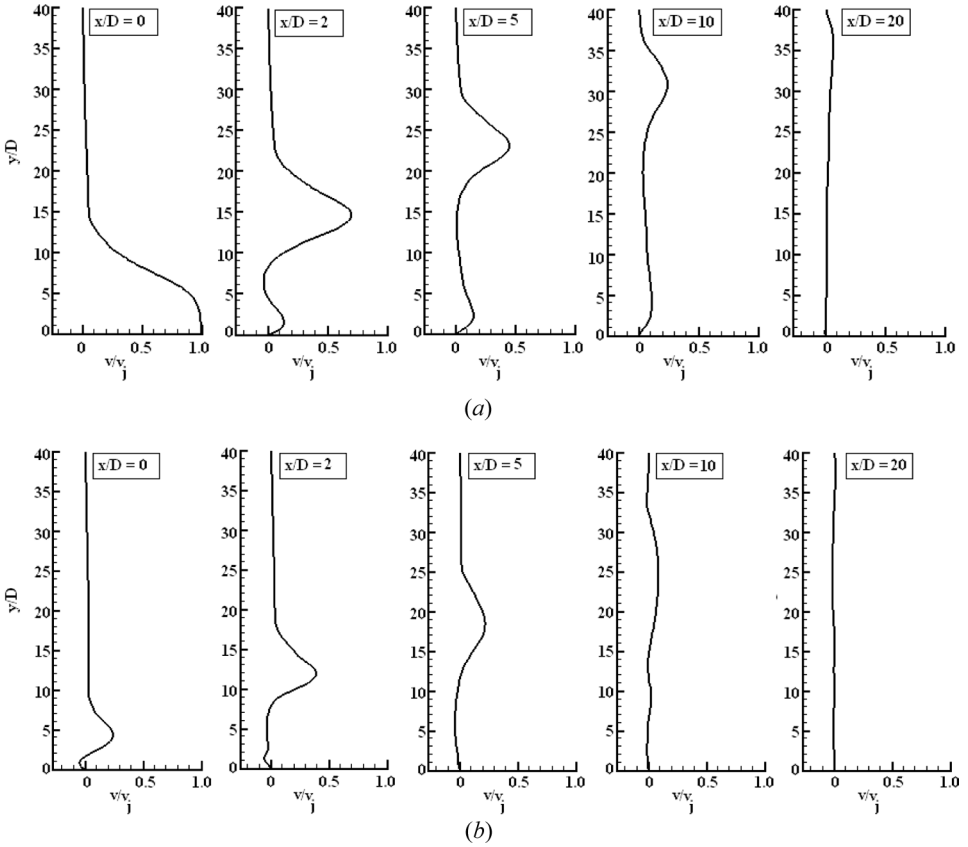


Figure 6. Prediction of vertical component of the mean velocity at different downstream locations for $R = 6$; (*a*) $z/D = 0$; (*b*) $z/D = 6$.

is formed near the bottom wall. Above this region a wakelike region starts at approximately $y/D = 3$ and moves away from the wall as one goes in the downstream direction. Farther downstream the jet becomes almost horizontal and runs parallel to the crossflow, showing quite small values of the vertical component. Changes of the vertical component profile at the transverse plane ($z/D = 6$) are observed as shown in Figure 6*b*. The velocity gradients ($\partial v/\partial y$) in the wall jet layer are smaller and the wake region is reduced. The vertical penetration height of the jet is observed to be reduced. This is due to the entrainment and mixing of the jet with the crossflow.

The vertical component of the mean velocity at two transverse planes ($z/D = 0$ and 6) and at different downstream locations for the velocity ratio $R = 9$ are shown in Figure 7. The peak values of the vertical component are observed at higher positions than for the case with $R = 6$. Thus the jet trajectory is greater in this case compared to the case with $R = 6$. The qualitative change of the velocity profiles at $z/D = 6$ are observed to be similar to those in the case of $R = 6$ (Figures 6*a* and 6*b*).

Downloaded By: [Dewan, Anupam] At: 05:36 15 April 2008

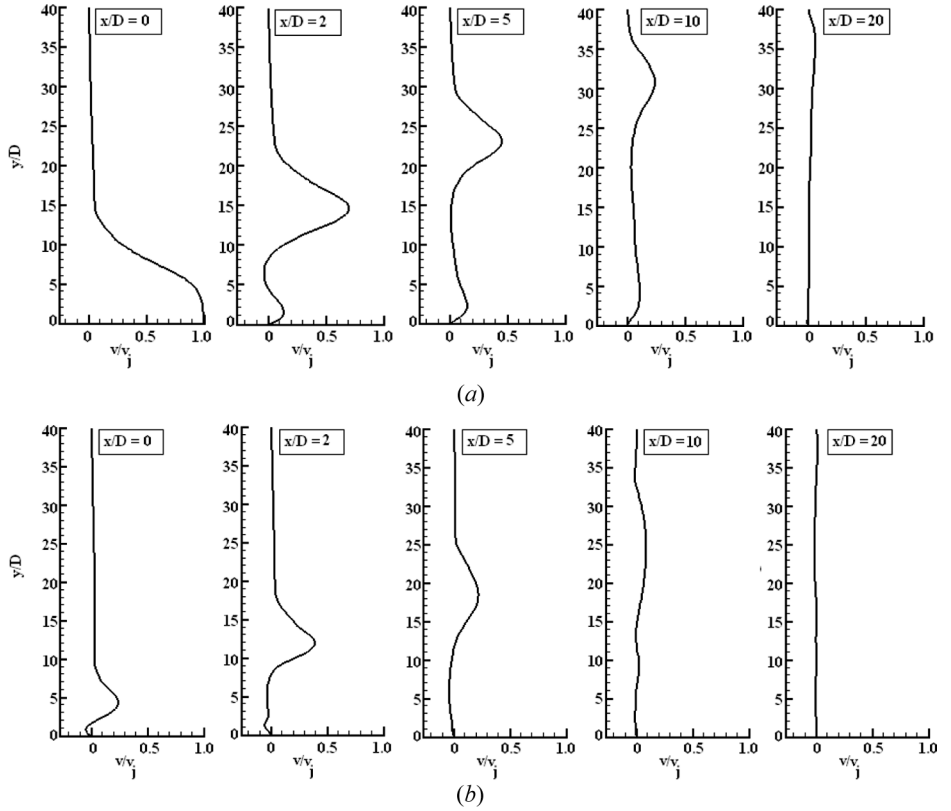


Figure 7. Prediction of vertical component of the mean velocity at different downstream locations for $R = 9$: (*a*) $z/D = 0$; (*b*) $z/D = 6$.

The flow three-dimensionality of the present problem can be demonstrated by showing the presence of transverse or spanwise components of the mean velocity in the flow field. Due to the symmetry of the flow about the jet central plane, the values of the transverse velocities at the jet central plane ($z/D = 0$) are found to be zero (not shown in figure). The variation of the transverse velocity at two different downstream positions and at different transverse planes ($z/D = 3$ and 6) are shown in Figure 8 for the velocity ratio $R = 6$.

The variations of the spanwise component of the velocity at the plane $z/D = 3$ and at different downstream locations are shown in Figure 8*a*. At the jet exit region ($x/D = 0$), a small value of the transverse component of velocity is observed at an approximate height of $y/D = 6$. Due to the presence of this small value, the jet acts toward the side wall after leaving the jet slot. Since the crossflow is relatively weaker than the jet, crossflow fluids on both sides of the jet spread slightly into the transverse direction after leaving the slot. Downstream of the jet exit region ($x/D = 2$), the formation of the counter-rotating vortex pair (CRVP) starts, and from this location, the transverse velocity is controlled by both the CRVP and the wake vortices. Behind the jet slot, a low-pressure region prevails in the flow field close

Downloaded By: [Dewan, Anupam] At: 05:36 15 April 2008

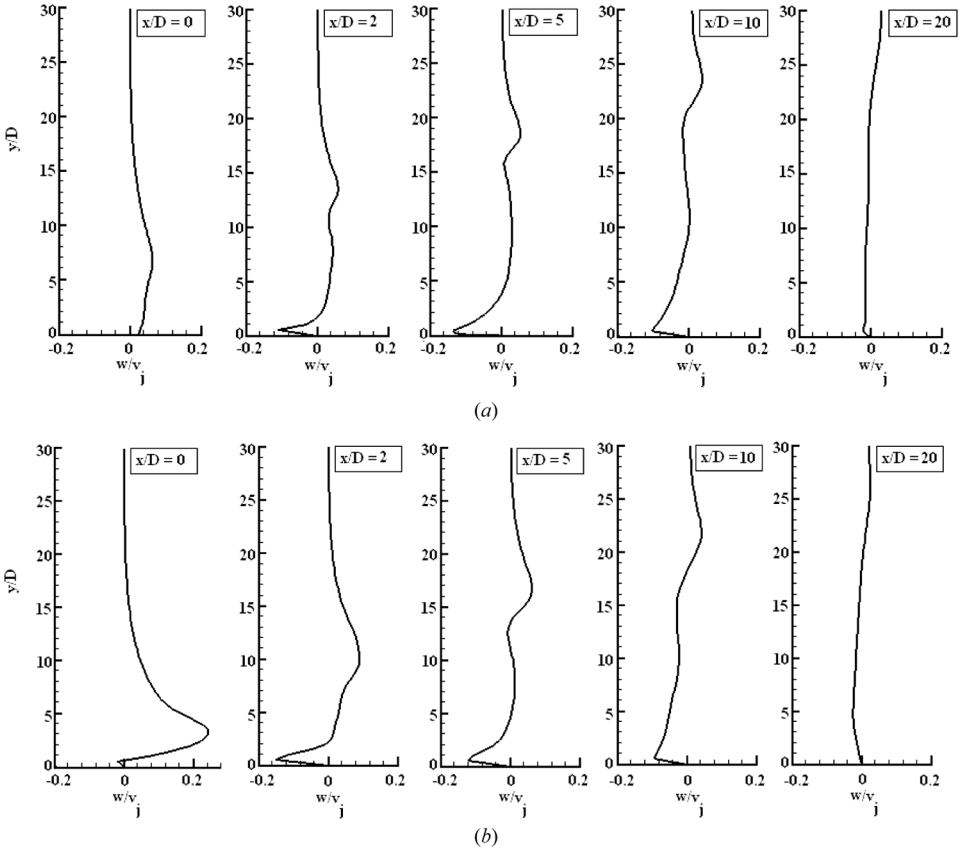


Figure 8. Prediction of spanwise component of mean velocity at different downstream locations for $R = 6$: (*a*) $z/D = 3$; (*b*) $z/D = 6$.

to the bottom wall, due to the wake effect. The low-pressure region induces surrounding fluid toward the center of the jet, close to the bottom wall. Thus the transverse component acts in the direction from the side wall toward the central vertical plane of the jet. The transverse velocities close to the bottom wall are reported at all the positions ($x/D = 2$, 5, 10, and 20) for two planes, $z/D = 3$ and 6. Moving away from the bottom wall, this variation is reduced.

The variations of the spanwise component of the velocity at the plane $z/D = 6$ are shown in Figure 8*b*. A reverse trend of the transverse component of the mean velocity is observed near the bottom wall at $z/D = 6$ and $x/D = 0$. The transverse velocity is toward the central vertical plane. At other downstream positions ($x/D = 2$, 5, 10, and 20), the profiles of the transverse component of the mean velocity are similar to those at the plane $z/D = 3$.

The variations of the spanwise velocity at two transverse planes and at different downstream locations are shown in Figure 9 for $R = 9$. In this case the spread of the jet at both sides (at $x/D = 0$) is observed to be greater compared to the case of $R = 6$ (Figures 8*a* and 8*b*). Downstream of the jet slot ($x/D = 2$), the spanwise velocity is

Downloaded By: [Dewan, Anupam] At: 05:36 15 April 2008

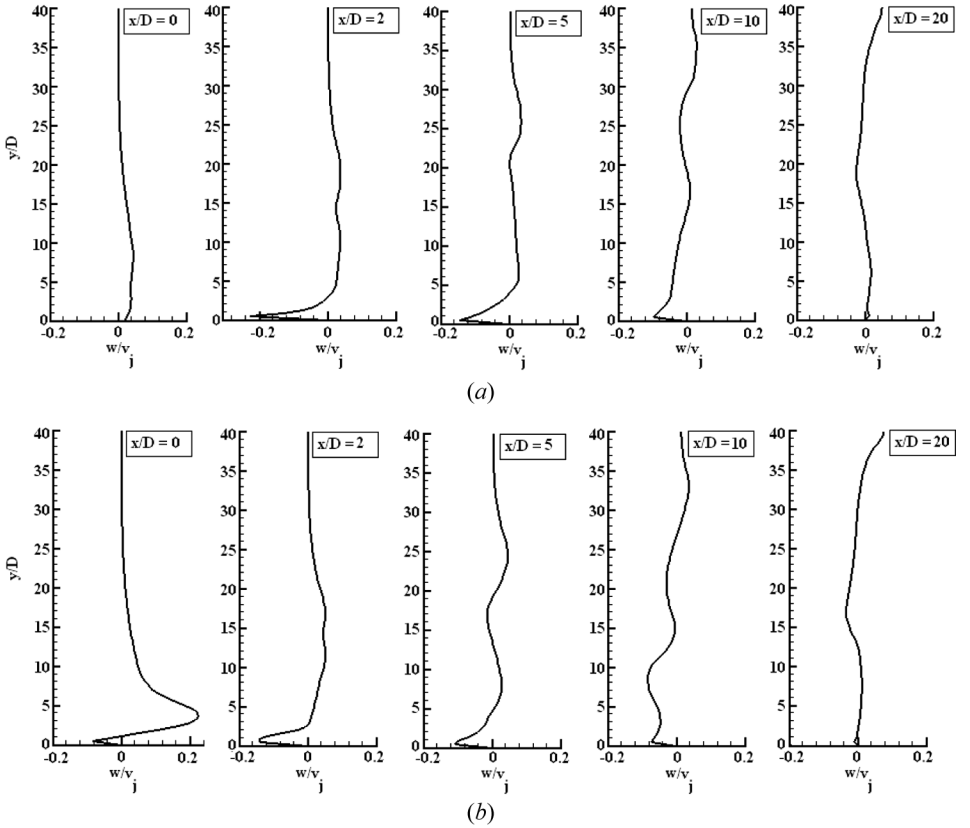


Figure 9. Prediction of spanwise component of mean velocity at different downstream locations for $R = 9$: (*a*) $z/D = 3$; (*b*) $z/D = 6$.

higher at both the transverse planes compared to the case with $R = 6$. Moreover, the flow reversals close to the bottom wall at $z/D = 6$ and at the position $x/D = 0$ are observed to be more prominent compared to the case with $R = 6$.

It is to be noted that the trends of the mean velocity profiles (u/v_j), (v/v_j), and (w/v_j) predicted so far in the present work resemble the trends of similar predictions for square jets in crossflow [20, 31, 33]).

3.2. Mean Temperature Field

It has already been explained that the jet is slightly heated (5.7°C for $R = 6$ and 6.1°C for $R = 9$). Due to the small temperature difference, the changes of density are assumed to be negligible and therefore the flow field is assumed to be unaffected by the temperature field. The temperature distribution can provide good information about the mixing behavior of the jet with the crossflow.

The variations of the normalized mean temperature with the vertical height (y/D) at different spanwise planes and at different downstream locations for the velocity ratio $R = 6$ are shown in Figure 10. At the jet exit region ($x/D = 0$), it is

Downloaded By: [Dewan, Anupam] At: 05:36 15 April 2008

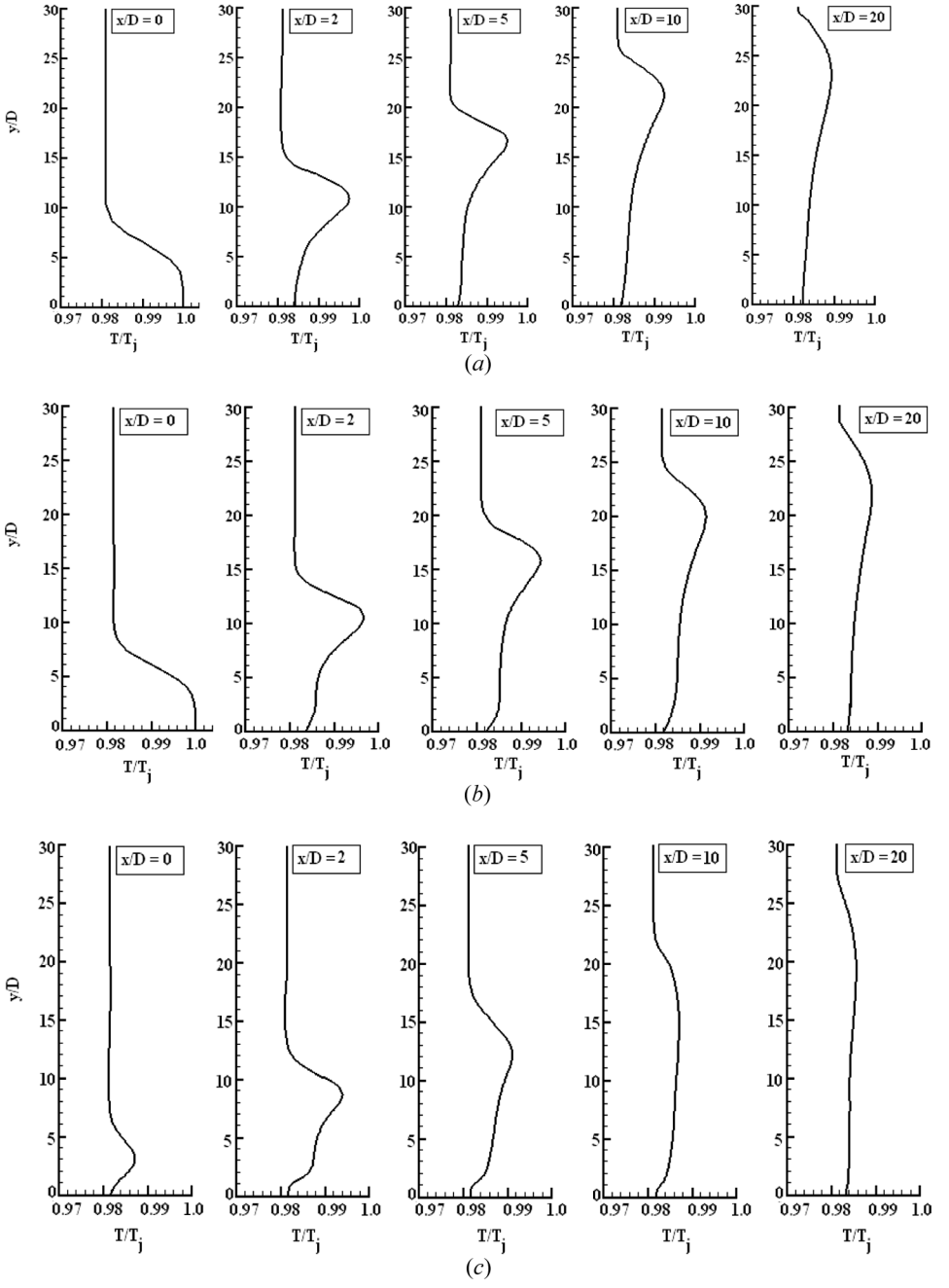


Figure 10. Prediction of the mean temperature at different downstream locations for $R = 6$: (*a*) $z/D = 0$; (*b*) $z/D = 3$; (*c*) $z/D = 6$.

Downloaded By: [Dewan, Anupam] At: 05:36 15 April 2008

observed that the peak of the mean temperature is near the wall, which indicates the high temperature of the jet stream at the jet inlet. Farther downstream the temperature peak moves upward along with the jet, and this spread is controlled by the velocity field. It is observed that upon moving away from the bottom wall, the value of the temperature gradually increases to a maximum or peak value and decreases monotonically thereafter. The distribution of the mean temperature at the upper and lower halves of the jet is different due to the fact that the distribution of the temperature in the lower half of the jet is controlled by the reverse flow. It is observed that the temperature profiles show similar trends as the vertical component of the mean velocity. This may be due to the fact that the prescribed boundary condition of the temperature at the jet inlet is similar to the vertical component of the mean velocity. It is also observed that though the jet is slightly heated compared to the crossflow, the decay rate of the temperature with downstream distance is quite small, due to a weak crossflow.

At the spanwise plane $z/D = 3$ (Figure 10*b*), the temperature profiles are quite similar to the profiles at the jet central plane ($z/D = 0$), due to the nonmixing and small interaction of the jet stream with the crossflow stream at this plane. The temperature distributions at the spanwise plane ($z/D = 6$) are significantly different from those at the first two planes ($z/D = 0$ and 3). At this plane the value of the temperature near the bottom wall at the jet exit region ($x/D = 0$) is observed to be smaller compared to that at the other spanwise planes ($z/D = 0$ and 3). From the temperature profiles at all spanwise planes, it can be concluded that the decay or dilution of the temperature along the spanwise direction is small compared to the corresponding decay in the cross-stream direction.

In the case of the velocity ratio $R = 9$, the temperature profile shows similar behavior (Figure 11) to that in the case of $R = 6$. In this case the peak values of the temperature occur at a higher vertical position compared to the case with $R = 6$. This is due to the higher trajectory and penetration of the jet compared to the case with $R = 6$. In this case also, the temperature distributions are different in the upper and lower halves. Moreover, the profiles are different at different spanwise planes. The spread of the temperature profiles is slightly less at the outer spanwise plane ($z/D = 6$) compared to the inner spanwise planes ($z/D = 0$ and 3). Since the jet is comparatively stronger, appreciable temperature peak values are obtained even at the far downstream positions at the outer spanwise plane ($z/D = 6$), which was not observed in the case of $R = 6$.

Isocontours of the mean temperature at the x–y plane and at three different spanwise planes ($z/D = 0$, 5, and 6) for $R = 6$ and 9 are presented in Figures 12*a* and 12*b*, respectively. The temperature contour shows shapes somewhat similar to the well-known Gaussian distribution. The mean temperature variations of the heated free jet are generally observed to be small [8]. Therefore all the temperature fluctuations in the crossflow jet may result from the mixing and the interaction between the jet and crossflow. In the upper part of the jet, the distribution of the contour is dense, thus indicating that the mixing between the jet and the crossflow is rather active. In contrast, relatively sparse contours are developed widely in the inner part of the jet. This originates from a low-velocity reverse flow region, which may promote the process of thermal spread in the inner part of the jet. The spread of the mean temperature is affected by the mean velocity field at different spanwise

Downloaded By: [Dewan, Anupam] At: 05:36 15 April 2008

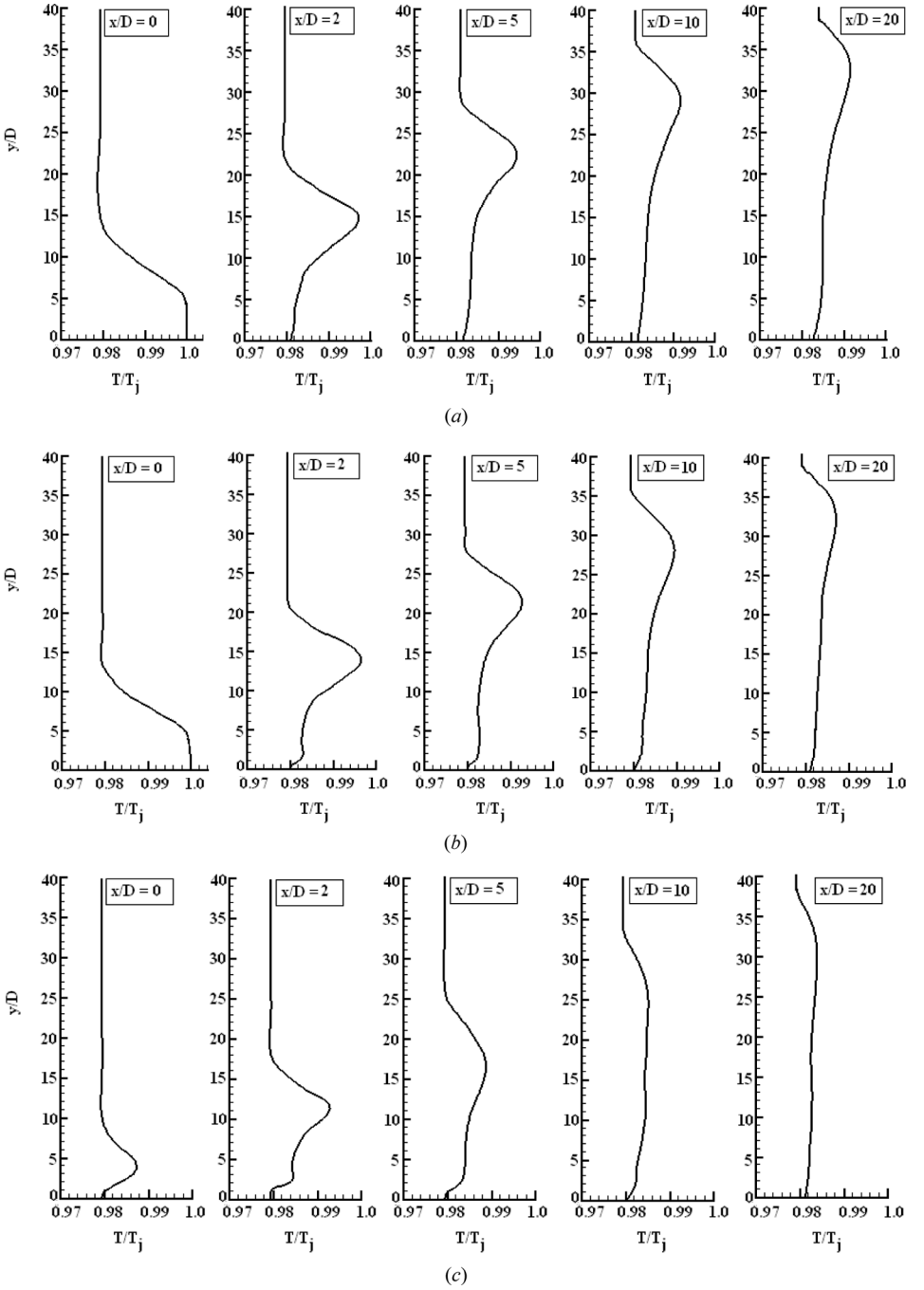


Figure 11. Prediction of mean temperature at different downstream locations for $R = 9$: (*a*) $z/D = 0$; (*b*) $z/D = 3$; (*c*) $z/D = 6$.

Downloaded By: [Dewan, Anupam] At: 05:36 15 April 2008

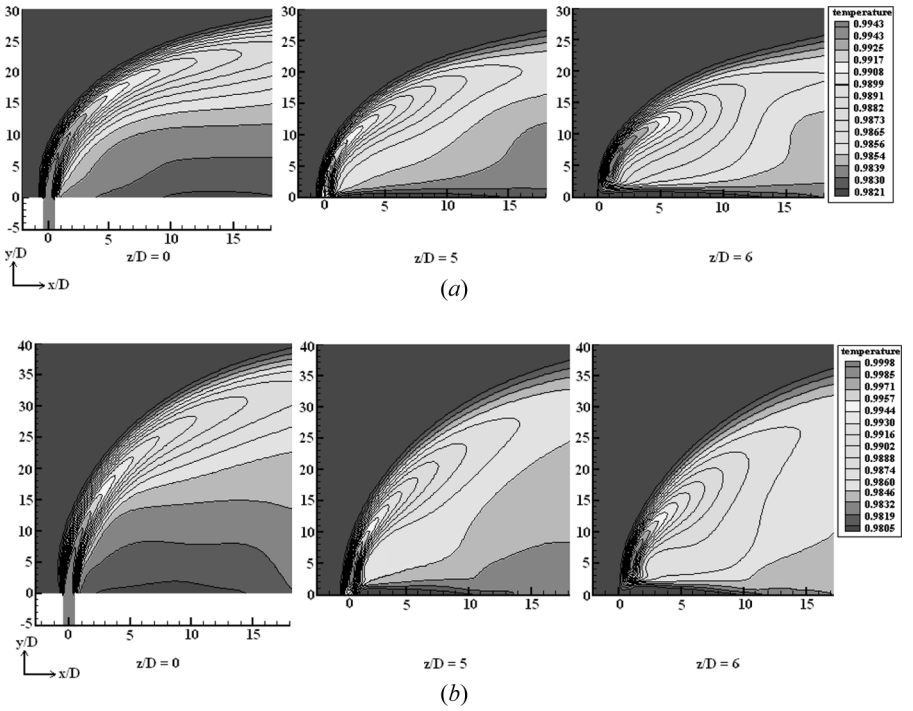


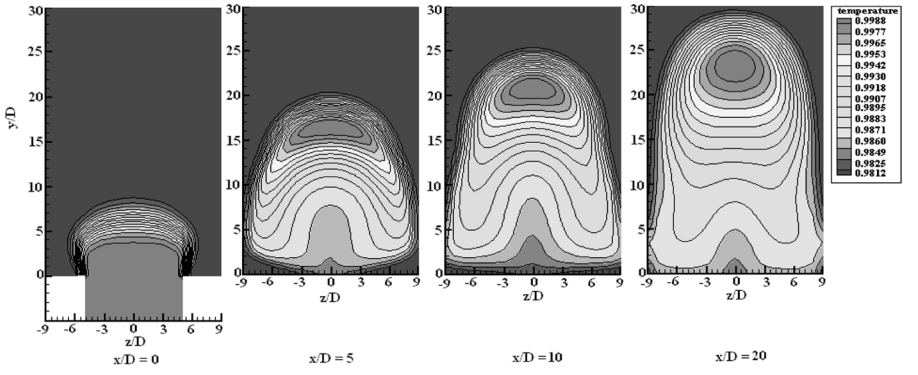
Figure 12. Mean temperature contours at three different spanwise (x–y) planes, $z/D = 0$, 5, and 6: (*a*) $R = 6$; (*b*) $R = 9$.

locations. At the edge and outside of the slot, the spread of the temperature is less compared to that at the center, which is similar to the case of the mean velocity field distribution.

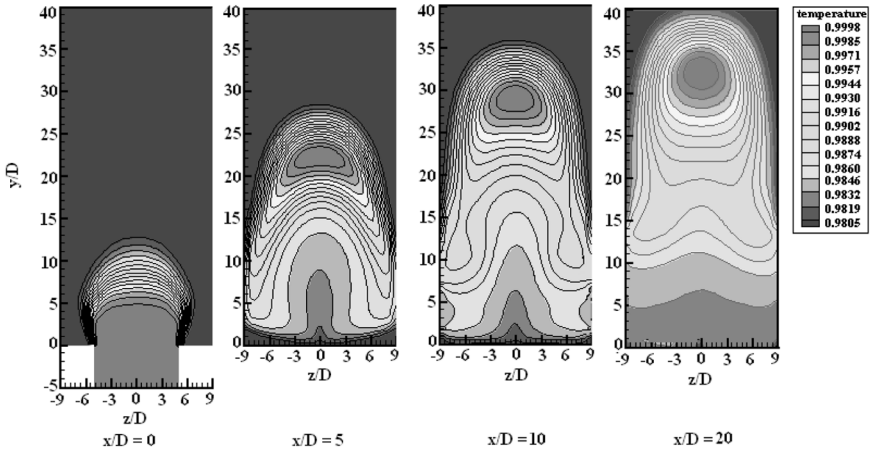
In case of $R = 9$ the jet is relatively stronger and therefore the spread of the temperature or the penetration of the temperature occurs up to a higher position than that in the case of $R = 6$ (Figure 12*b*). The temperature distribution follows the mean velocity distribution in this case also.

Figures 13*a* and 13*b* show the mean temperature contours at various y–z planes and at different downstream locations for the velocity ratios $R = 6$ and 9. The spread of the high-temperature jet core due to the interaction of the jet with the crossflow can be understood from these plots. The high-temperature jet fluid enters from the jet slot and, after interaction with the crossflow, this zone moves upward along with the downwash from the crossflow. It is observed that in the upper part of the jet, the distribution of the contour is dense, whereas a quite coarse and relatively wide temperature distribution occurs in the inner part of the jet. The shape of the temperature distribution is more or less circular immediately downstream of the slot, and it becomes kidney-shaped farther downstream. It is observed that the counter-rotating vortex dynamics controls the temperature distribution. At all locations, the shape is observed to be symmetric about the central vertical plane ($z/D = 0$).

Downloaded By: [Dewan, Anupam] At: 05:36 15 April 2008



(*a*)



(*b*)

Figure 13. Mean temperature contours at various y–z planes, $x/D = 0$, 5, 10, and 20: (*a*) $R = 6$; (*b*) $R = 9$.

In the case of the velocity ratio $R = 9$ the y–z plane mean temperature contours (Figure 13*b*) show a similar trend as in the case of $R = 6$, but far downstream the contours show some differences. At $x/D = 10$, the isotherm pattern near the bottom corners show some dissimilarity from those for $R = 6$. At the position $x/D = 20$, sharp variations in the temperature are confined to the upper part of the flow field, and variations in the bottom part and near the wall are small. This also occurs due to the position of the counter-rotating vortex in the upper part of the flow field at that location.

The mean temperature contours are presented in Figure 14 for three heights ($y/D = 1$, 5, and 10) in the x–z plane for the velocity ratio $R = 6$ and 9. It is observed that as the height increases, the maximum of the temperature moves downstream from the jet and the temperature is distributed over a large region. Dispersion of the temperature is influenced by the wake vortices formed in the x–z plane. The temperature

Downloaded By: [Dewan, Anupam] At: 05:36 15 April 2008

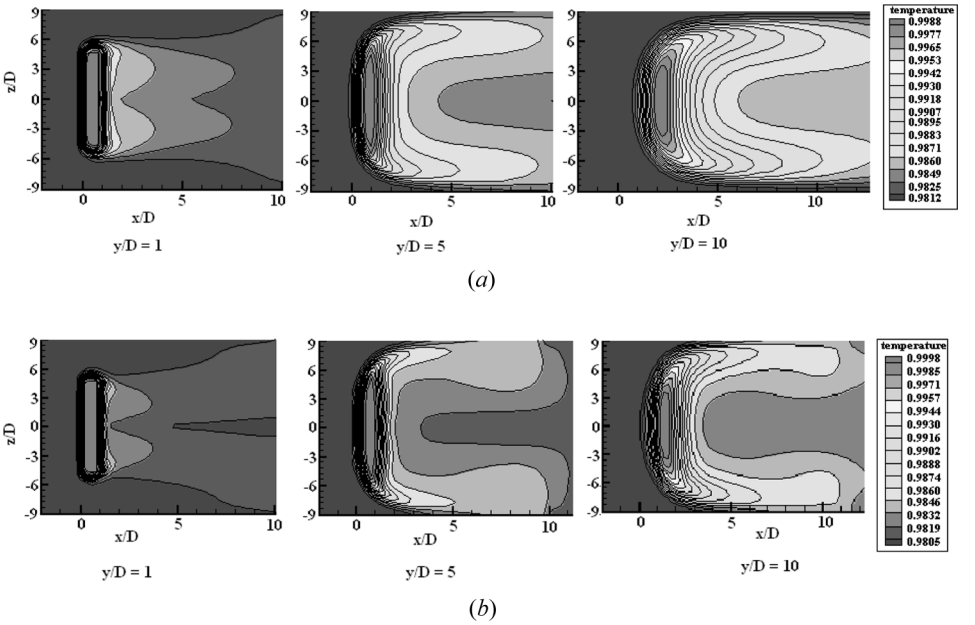


Figure 14. Mean temperature contours at various x–z planes at different y/D locations: (*a*) $R = 6$; (*b*) $R = 9$.

distribution at different planes observed in the present work is similar to that reported by Shi et al. [12] and by Said et al. [13]. In the case of the velocity ratio $R = 9$, also, the wake vortices control the temperature distribution, which is shown in Figure 14*b*.

From the plots of the velocity components and temperature distributions, it is observed that both the velocity and temperature fields exhibit three-dimensional nature.

3.3. Comparison with Measurements

A comparison of the predicted results of the mean temperature with the experimental data of Ramaprian and Haniu [4] and of Haniu and Ramaprian [5] is presented in this section. The results are presented in the s–n coordinate system.

The normalized excess temperature profile $(\Delta T/\Delta T_j)$, where $\Delta T = T - T_a$ and $\Delta T_j = T_j - T_a$, in the jet central vertical plane $(z/D = 0)$ at four downstream positions for the velocity ratio $R = 6$ is shown in Figure 15. The temperature field is slightly overpredicted. The agreement between the present predictions and the experimental data is observed to be better in the near field ($s/D = 4.94$ and 9.68) compared to the far field ($s/D = 18.86$ and 28.12). In the case of the velocity ratio $R = 9$ (Figure 16), the prediction shows the same behavior as the experimental data, but it overpredicts more at the far downstream location ($s/D = 29.73$) compared to the similar location in the case of $R = 6$ (Figure 15). Overall, the present predictions show reasonably good agreement with the experimental data.

Downloaded By: [Dewan, Anupam] At: 05:36 15 April 2008

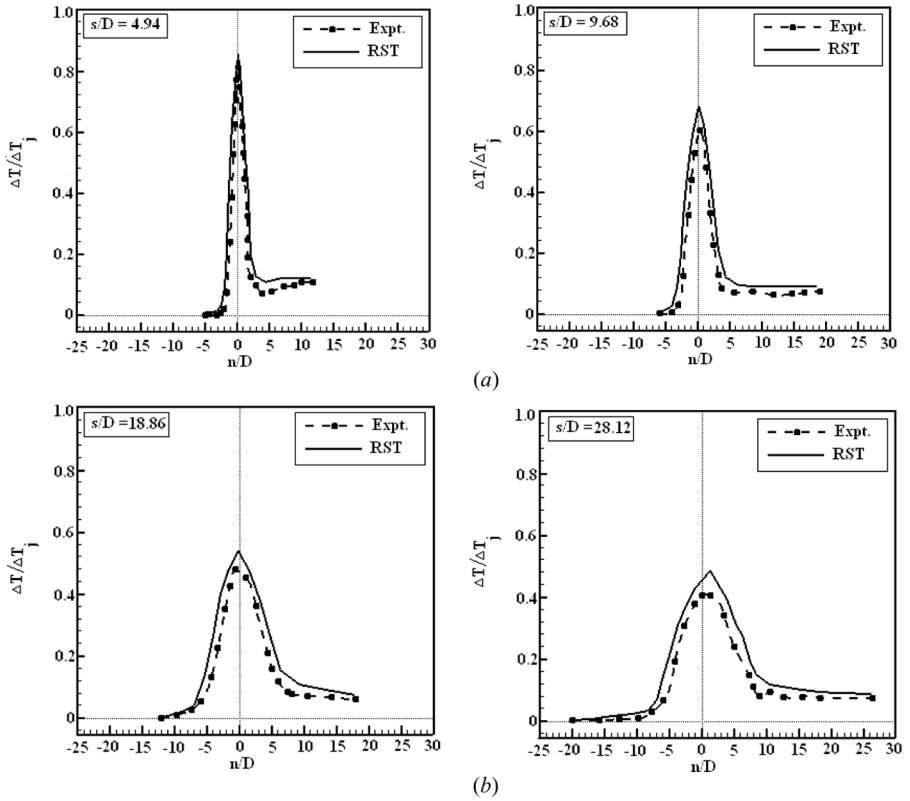


Figure 15. Comparison of normalized excess temperature at jet central plane ($z/D = 0$) for $R = 6$: (*a*) $s/D = 4.94$ and 9.68; (*b*) $s/D = 18.86$ and 28.12.

4. CONCLUSIONS

The flow field of a slightly heated rectangular jet discharged into a narrow channel crossflow has been investigated numerically using the Reynolds stress transport model. The various terms of the Reynolds stress transport equation that need modeling are modeled based on proposals in the literature that are suitable for the present flow configuration. The effect of the buoyancy on the flow field is negligible, due to a small temperature difference, so that the temperature is treated as a passive scalar, and good agreement with the experiments demonstrates the validity of this assumption. The effect of the velocity ratio on the flow field and temperature distribution are discussed for two velocity ratios, $R = 6$ and 9. The higher velocity ratio is characterized by higher jet trajectories and temperature trajectory compared to that for $R = 6$. The mean temperature field in the case of the heated jet appears to be closely linked to the mean velocity field, and the distribution of the temperature is controlled by the different vortices formed in the flow field. The temperature dispersion observed in the present investigation is consistent with similar results reported in the literature. The overall thermal characteristics obtained

Downloaded By: [Dewan, Anupam] At: 05:36 15 April 2008

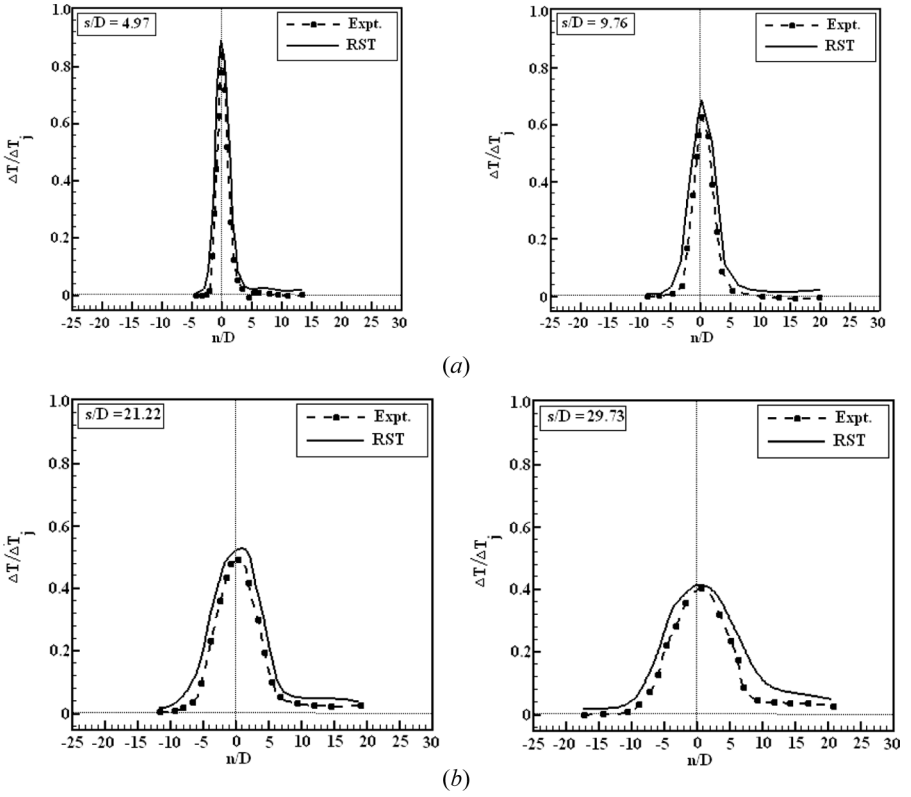


Figure 16. Comparison of normalized excess temperature at jet central plane ($z/D = 0$) for $R = 9$: (*a*) $s/D = 4.97$ and 9.76; (*b*) $s/D = 21.22$ and 29.73.

with the RST model are in reasonably good agreement with the experimental data. The present investigation establishes the three-dimensionality of the flow field, which is in some contrast to the observation made by Ramaprian and Haniu [4] and Haniu and Ramaprian [5], who perhaps did not find it necessary to carry out a detailed 3-D experimental investigation.

REFERENCES

1. T. F. Fric and A. Roshko, Vortical Structures in the Wake of a Transverse Jet, *J. Fluid Mech.*, vol. 279, pp. 1–47, 1994.
2. R. M. Kelso, T. T. Lim, and A. E. Perry, An Experimental Study of Round Jets in Cross-flow, *J. Fluid Mech.*, vol. 306, pp. 111–144, 1996.
3. L. L. Yuan, R. L. Street, and J. H. Ferziger, Large Eddy Simulations of a Round Jet in Crossflow, *J. Fluid Mech.*, vol. 379, pp. 71–104, 1999.
4. B. R. Ramaprian and H. Haniu, Turbulence Measurement in Plane Jets and Plumes in Cross Flow, Tech. Rep. 266, IIHR, University of Iowa, Iowa City, IA, USA, 1983.
5. H. Haniu and B. R. Ramaprian, Studies on Two-Dimensional Curved Nonbuoyant Jets in Cross Flow, *Trans. ASME, J. Fluids Eng.*, vol. 111, pp. 78–86, 1989.

Downloaded By: [Dewan, Anupam] At: 05:36 15 April 2008

6. C. E. Wark and J. F. Foss, Thermal Measurement for Jets in Disturbed and Undisturbed Crosswind Conditions, *AIAA J.*, vol. 26, pp. 901–902, 1988.
7. K. S. Chen and J. Y. Hwang, Experimental Study on the Mixing of One and Dual-Line Heated Jets with a Cold Crossflow in a Confined Channel, *AIAA J.*, vol. 293, pp. 353–360, 1991.
8. S. A. Sherif and R. H. Pletcher, Jet-Wake Thermal Characteristics of Heated Turbulent Jets in Crossflow, *J. Thermophys.*, vol. 5, pp. 181–191, 1991.
9. H. Nishiyama, T. Ota, M. Hamada, and Y. Takahashi, Temperature Fluctuations in a Slightly Heated Slot Jet Issuing into a Crossflow, *Exp. Thermal Fluid Sci.*, vol. 6, pp. 252–262, 1993.
10. S. Sarkar and T. K. Bose, Comparison of Different Turbulence Models for Prediction of Slot-Film Cooling: Flow and Temperature Field, *Numer. Heat Transfer B*, vol. 28, pp. 217–238, 1995.
11. R. R. Hwang and T. P. Chiang, Numerical Simulation of Vertical Forced Plume in a Crossflow of Stably Stratified Fluid, *Trans. ASME, J. Fluids Eng.*, vol. 117, pp. 696–705, 1995.
12. Y. Shi, M. B. Ray, and A. S. Mujumdar, Numerical Study on the Effect of Cross-flow on Turbulent Flow and Heat Transfer Characteristics under Normal and Oblique Semi-confined Impinging Slots Jets, *Drying Technol.*, vol. 21, pp. 1923–1939, 2003.
13. N. M. Said, H. Mhiri, S. E. Golli, G. L. Palec, and P. Bournot, Three-Dimensional Numerical Calculations of Jet in an External Cross Flow: Application to Pollutant Dispersion, *Trans. ASME, J. Heat Transfer*, vol. 125, pp. 510–522, 2003.
14. C. E. Niederhaus, F. H. Champagne, and J. W. Jacobs, Scalar Transport in a Swirling Transverse Jet, *AIAA J.*, vol. 35, pp. 1697–1704, 1997.
15. S. H. Smith and M. G. Mungal, Mixing Structure and Scaling of the Jet in Crossflow, *J. Fluid Mech.*, vol. 357, pp. 83–122, 1998.
16. L. K. Su and M. G. Mungal, Simultaneous Measurement of Scalar and Velocity Field Evolution in Turbulent Crossflowing Jets, *J. Fluid Mech.*, vol. 513, pp. 1–45, 2004.
17. M. W. Plesniak and D. M. Cusano, Scalar Mixing in a Confined Rectangular Jet in Cross-flow, *J. Fluid Mech.*, vol. 524, pp. 1–45, 2005.
18. J. W. Shan and P. E. Dimotakis, Reynolds-Number Effects and Anisotropy in Transverse-Jet Mixing, *J. Fluid Mech.*, vol. 566, pp. 47–96, 2006.
19. S. V. Patankar, D. K. Basu, and S. A. Alpay, Prediction of Three-Dimensional Velocity Field of a Deflected Turbulent Jet, *Trans. ASME, J. Fluids Eng.*, vol. 99, pp. 758–762, 1977.
20. K. Kalita, A. Dewan, and A. K. Dass, Prediction of Turbulent Plane Jet in Crossflow, *Numer. Heat Transfer A*, vol. 41, pp. 1–12, 2002.
21. R. Keimasi and T. Rahni, Numerical Simulation of Jets in a Crossflow Using Different Turbulence Models, *AIAA J.*, vol. 39, pp. 2268–2277, 2001.
22. A. O. Demuren, Characteristics of Three-Dimensional Turbulent Jets in Crossflow, *Int. J. Eng. Sci.*, vol. 31, pp. 899–913, 1993.
23. C. A. Hale, M. W. Plesniak, and S. Ramadhyani, Structural Features and Surface Heat Transfer Associated with a Row of Short-Hole Jets in Cross-flow, *Int. J. Heat Fluid Flow*, vol. 21, pp. 542–553, 2000.
24. G. Biswas and V. Eswaran (eds.), *Turbulent Flows Fundamentals, Experiments and Modeling*, Narosa, Delhi, India, 2002.
25. F. S. Lien and M. A. Leschziner, Assessment of Turbulent Transport Models including Nonlinear RNG Eddy-Viscosity Formulation and Second Moment Closure, *Comput. Fluids*, vol. 23, pp. 983–1004, 1994.
26. C. G. Speziale, S. Sarkar, and T. B. Gataski, Modelling the Pressure-Strain Correction of Turbulence: An Invariant Dynamical Systems Approach, *J. Fluid Mech.*, vol. 227, pp. 245–272, 1991.

27. S. Sarkar and L. Balakrishnan, Application of a Reynolds-Stress Transport Model to the Compressible Shear Layer, ICASE, Rep. 90–18, NASA CR 182002, 1990.
28. H. K. Versteeg and W. Malalasekera, *An Introduction to Computational Fluid Dynamics the Finite Volume Method*, 2nd ed., pp. 70–72, Addison Wesley Logman, Harlow, England, 1996.
29. A. Hoda, S. Acharya, and M. Tyagi, Reynolds Stress Transport Model Predictions and Large Eddy Simulations for Film Coolant Jet in Crossflow, Paper 2000-GT-0249, ASME Int. Gas Turbine Conf., Munich, 2000.
30. B. J. Daly and F. H. Harlow, Transport Equations in Turbulence, *Phys. Fluids*, vol. 13, pp. 2634–2649, 970.
31. A. Hoda and S. Acharya, Predictions of a Film Coolant Jet in Crossflow with Different Turbulence Models, *Trans. ASME, J. Turbomach.*, vol. 122, pp. 558–569, 2000.
32. J. Andreopoulos and W. Rodi, Experimental Investigation of Jets in a Cross-flow, *J. Fluid Mech.*, vol. 138, pp. 93–127, 1984.
33. P. Ajersch, S. Ketler, J. M. Zhou, I. Gartshore, and M. Salcudean, Multiple Jets in Cross-flow: Measurements and Numerical Simulations, *Trans. ASME, J. Turbomach.*, vol. 119, pp. 330–342, 1997.

Downloaded By: [Dewan, Anupam] At: 05:36 15 April 2008